MEMS-Fabricated Micro Vacuum Electron Devices (μVEDs) for Terahertz (THz) Applications

Young-Min Shin, Larry R. Barnett, and Neville C. Luhmann Jr.
Department of Applied Science, University of California, Davis, CA 95616, USA

***Abstract*— New types of micro vacuum electron devices (μVEDs) for high power and broadband applications in the THz and sub-THz regimes are presented. We have developed advanced MEMS techniques permitting the fabrication and on-chip integration of μVED circuit elements based on photolithography and chemical etching.**

I. INTRODUCTION

THE high power capability and high energy conversion efficiency of vacuum electron devices (VEDs) have attracted considerable attention in the THz community which requires a compact high power radiation source for large signal-to-noise-ratio (SNR) applications including imaging, telecommunications, diagnostics, and radar systems. This approach requires linear scale-down of bulky VED elements, which necessitates the microfabrication of the associated electronic circuits resulting from the fact that as the frequency increases conventional mechanical machining becomes problematic in building micro-features owing to technical limitations of tolerance, accuracy, tool-size, and surface roughness. Also, conventional electronic circuit structures are highly lossy and dispersive in the THz and sub-THz regime owing to severe ohmic losses, so that the radiation intensity steeply falls off proportional to $1/f^2$, where f is the operating frequency, with narrowing the instantaneous bandwidth. Breakthroughs addressing this issue have been proposed from the invention of various high frequency electronic circuits and the rapid advance of MEMS technology. This paper presents innovative lithography and etching techniques compatible with μVED circuit structures, which are investigated for the development of highly efficient and wideband THz and sub-THz radiation sources.

II. NOVEL MILLIMETER/SUBMILLIMETER VEDS

The main focus of our THz μVED development has been to conceive thermally and mechanically robust all-metal-electronic circuits, which efficiently induce intensive surface waves (plasmonic waves) covering a broad frequency spectrum and which are compatible with microfabrication techniques.

A new class of Smith-Purcell radiation free electron laser (SPR FEL) using counter-streaming electron beams (CSEBs) on a one-dimensional hole-array[1 – 3] was previously invented by one of the authors (Young-Min Shin). The FDTD-PIC simulation results of the plasmonic device show that the radiation intensity of the CSEBs-SPR is approximately two orders of magnitude higher than that of conventional single-beam SPR (SB-SPR) over the frequency spectrum up to 0.6 THz. Also, the stimulated emission current density threshold (~50 A/cm^2) of the CSEB-SPR is considerably lower than that (~150 A/cm^2) of the SB-SPR, which implies that the radiation mechanism using the CSEBs is effective in lowering the transition threshold.

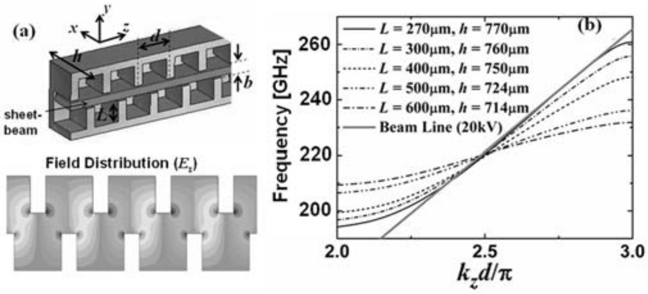

Fig. 1. (a) 3D Schematics and axial field (E_Z) distributions of high efficiency interaction RF-circuit with dimensional parameters of the structure (b) cold dispersion curves of the fundamental mode for various combinations of the dimensional parameters, L and h, at the 1st spatial harmonic regime (n = 1)

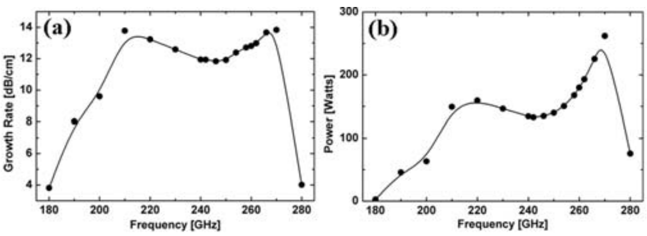

Fig. 2. (a) Linear growth rate and (b) saturated output power obtained from a frequency sweep with PIC simulations

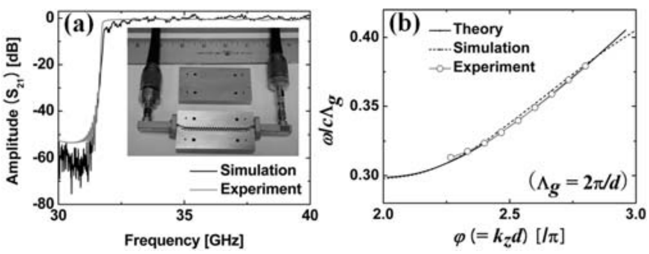

Fig. 3. Theoretical, numerical, and experimental analysis results of Ka-band BS circuit for proof-of-concept (a) rf-transmission data (S_{21}: simulation and experiment) of cold-test circuit (inset) (b) normalized dispersion curves from theory, simulation, and experiment.

The half-period staggering of a pair of one-dimensional vane array[4 – 6], the so-called "Barnett-Shin (BS) slow wave structure", allows the fundamental mode to have a strong symmetric axial electric field distribution (in-phase field variation) along the electron beam propagation direction. As shown in Fig. 1(a), the first mode of the staggered vane structure has a symmetric field distribution, which has sinusoidal phase variation along the axial direction. The input signal can thus be efficiently amplified under fundamental mode operation. At the center frequency of 220 GHz, we define the design parameters as φ (= $k_z d$) = 2.5π for phase synchronism with the 20 kV electron beam. The geometrical circuit dimensions designed for the first spatial harmonic operation (n = 1), provide broad bandwidth and sufficient

978-1-4244-2120-6/08/$25.00©IEEE.

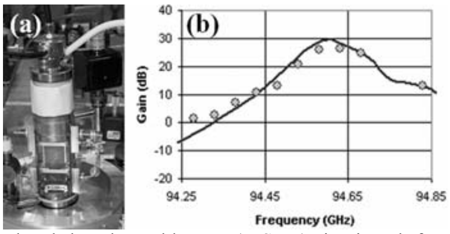

Fig. 4. (a) W-band sheet beam klystron (WSBK) circuit and rf-test setup and (b) 1D simulated (solid line) and measured (dotted line) gain curves

intrinsic volume for the beam-wave interaction. Figure 1(b) shows dispersion curves corresponding to various combinations of L and h while maintaining 220 GHz operation frequency and 2.5π synchronism. Note that the circuit dispersion increases with an increase of L and decrease of h. The design values of L and h are 270 μm and 770 μm respectively, which provide wide matching with the beam line. Figure 2(a) shows PIC simulation results varying input driving frequency (P_{in} = 50mW) with a short pulse white noise (Δt ~ 2ps). The growth rate exceeds 10 dB/cm over the 200 – 270 GHz frequency range, which corresponds to a hot bandwidth of 70 GHz (30%) actually spanning both the first and second passbands. The saturated output power is also plotted in Fig. 2(b). The efficiency at 220 GHz is 3.2% and the overall device efficiency can be further increased by use of a depressed collector. The rf response characteristic (proof-of-concept) of this device is experimentally examined in Ka-band in comparison with theory and simulation. Figure 3(a) shows that the measured transmission loss of the CNC-machined Ka-band circuit is about 0.5dB over 14 periods, which corresponds to only 0.012dB/cm attenuation (lossless). In Fig. 3(b), the dispersion curve from this measured S_{11} spectrum is very well agreed with simulation and theory, which experimentally proves practical application of the device concept to 220GHz.

The multi-cavity sheet beam klystron[7] is designed for W-band applications. Figure 4(a) illustrates a mechanically machined interaction circuit with 8 cavities, which consist of single-gap, 3-gap, and 7-gap for input, intermediate, and output cavities, respectively. The small signal analysis theoretically showed that the resonating circuit has 30dB gain over a bandwidth of 0.3GHz centered at 94.5GHz. Also, this device produced output power of 50kW on simulation and ≥10 kW on experiment. We are currently modifying its output cavity structure for quasi-optical coupling and microfabricating the electronic circuit using various MEMS approaches.

III. MICROFABRICATION

Present conventional machining technology allows a tolerance of over 5 μm and a surface roughness of a few hundred to a few thousand nanometers, which are the primary obstacles confronted by higher-power devices in the millimeter and submillimeter region. Furthermore, the smallest dimension of the circuit feature is restricted by the machining tool size. The demand for tight tolerances and high accuracy has thus led us to concentrate on state-of-the-art MEMS technologies and to create new ideas for 3D circuit construction.

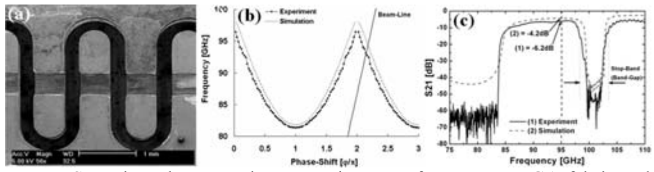
Fig. 5. Scanning electron microscope images of two-step LIGA-fabricated (a) folded waveguide and (b) coupled cavity (c) dispersion curve obtained from measured reflection scattering parameter (S11) from experiment and simulation

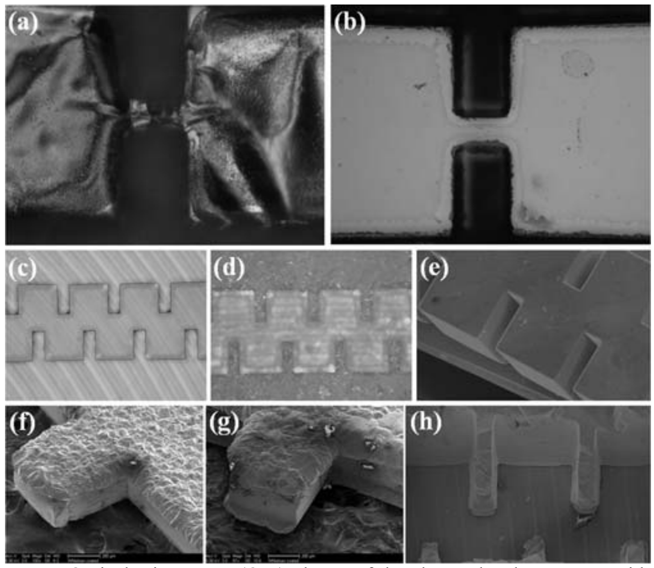
Fig. 6. Optical microscope (OM) photos of the electroplated structures with 120μm thick (a) SU8 (right) and (b) KMPR (left) molds after stripped by mold removers (DMSO, remover PG, and remover K) (c) - (h) OM and SEM images of 300 ~ 500μm thick KMPR molds and electroplated circuit structures.

One of the authors (Young-Min Shin) previously developed a two-step LIGA process[8],[9], where LIGA stands for Lithographie, Galvanoformung Abformung (lithography, electroplating, and molding) in German acronym, for building a complete 3D circuit structure. The two-step LIGA process consists of repetition of the entire LIGA procedure such as exposure, development, electroplating, and surface-finish (lapping and polishing) including additional alignment between the first and the second layers. The first layer is for forming the circuit geometry without a beam tunnel and the second layer is for forming a beam tunnel. Figure 5(a) exhibits the magnified images obtained by scanning electron microscope (SEM) of two-step LIGA fabricated circuits with beam tunnels. The circuit in Figs. 5(a) preserves very accurate dimensions including a rectangular beam tunnel. The tolerance of the completed circuits measured by SEM is less than 2 μm, which is much less than the tolerance, over 5 μm, of typical electrical discharge machining (EDM). Misalignment between the first and second layers is measured to be about 2 – 3 μm by an alignment method using cross-shaped micropinholes. Reflection scattering matrices (S_{11}) are measured in the folded waveguide structures at near 100 GHz using a vector network analyzer. The experimental dispersion curve from S_{11} in Fig. 5(b) is in agreement with simulations within 1.4% and the transmission loss in Fig. 5(c) of the circuit is about 6 dB,

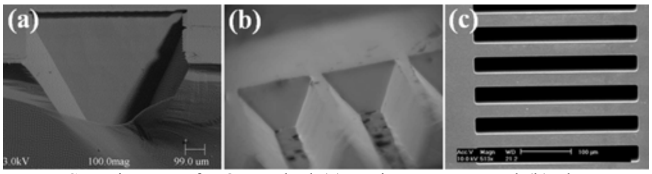

Fig. 7. SEM images of KOH-etched (a) cavity structure and (b) slow wave electronic circuit (c) DRIE-fabricated 1D-trasmission grating array structure.

which corresponds to 54 dB/m attenuation.

Normally, the LIGA process has utilized x-rays as an exposure light source since they have large penetration depth. However, a large synchrotron facility is requisite for the high intensity x-ray exposure, which makes the entire process complicated and time-consuming. Recently, ultraviolet (UV) lithography has been used for the LIGA process as an alternative to simplify the fabrication procedure. However, it is extremely difficult to remove exposed/cross-linked photoresist mold (SU-8) from the electroplated metal networks. Therefore, we have investigated a novel high aspect ratio lithography (HARL) technique using a new photoresist, KMPR, to overcome the disadvantages of the x-ray and conventional UV LIGA processes. Figures 6(a) and (b) show optical microscope (OM) images of the electroplated copper structures with 120 μm thickness after stripping SU8, (a), and KMPR, (b), molds. It should be noted that the KMPR mold is completely dissolved and removed, whereas the SU8 mostly remains and sticks to the copper structure. The result demonstrates that the crosslinked polymer resin can be removed from the metal structure by a standard removal process based on readily obtainable solvents. Figures 6(c) – (h) contains OM and SEM photos of KMPR molds and copper specimens electroplated on the KMPR-mold of 300 ~ 500 μm thickness. It should be noted that it might be challenging to form the KMPR mold exceeding 500 μm in a single-step UV LIGA process. Formation of the ultra-thick and high aspect ratio photoresist mold and its feasible and stable removal from the metallic network are underway.

The most well known silicon etching techniques are KOH-etching and deep reactive ion etching (DRIE). As shown in Fig. 7(a), the KOH-etching provides extremely smooth surfaces along the (111) crystal plane of silicon wafers and 54.7° tilt sidewalls which improve the circuit interaction impedance. Figure 7(b) shows the KOH-etching fabricated Smith-Purcell radiation (SPR) free electron laser (FEL) circuit. The DRIE can make very narrow trenches with high aspect ratio, which is applicable to planar slow wave structures. Figure 7(c) shows the plasmonic slow wave structure fabricated by DRIE.

IV. Surface Roughness Measurement

To more quantitatively assess possible applications of the LIGA process in the millimeter and submillimeter wave region, we measure the surface roughness, $\delta = \sqrt{2/\omega\mu\sigma}$, of LIGA-fabricated samples. When the surface roughness of the circuit is larger than the skin depth, the electromagnetic wave hardly propagates through waveguide structures, which makes it difficult to form the proper coupling and resonance in the circuit structure due to the lossy surface.

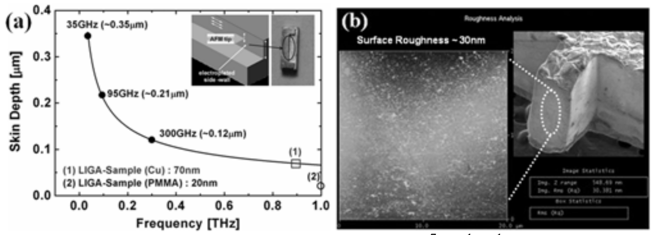

Fig. 8. (a) Calculated skin depth (σ = $5.8\times10^{7}[\Omega^{-1}m^{-1}]$) and measured surface roughness of x-ray LIGA samples (inset: PMMA mold and Cu block) (b) Surface roughness (~ 30nm, rms) on the sidewall of UV LIGA fabricated sample (inset)

In Fig. 8(a), surface roughness of x-ray LIGA samples (PMMA mold and Cu block) measured by atomic force microscope (AFM) ranges from 20 nm to 70 nm, which is much smaller than those, a few hundred to a few thousand nanometers, of typical EDMs. Figure 8(b) shows the AFM-measured surface profile on an 800 μm thick UV LIGA (KMPR) fabricated circuit side wall. The locally measured surface roughness is about 30 nm (rms), which is significantly smoother than that of the chemically and mechanically treated metal surface. Thus, LIGA processes using these chemically soluble photoresists are very advantageous and effective in fabricating metallic microstructures with nano-scale surface roughness, which can be utilized in the THz and sub-THz region.

V. Summary and Conclusion

In summary, we have theoretically, numerically, and experimentally verified rf-responses and radiation performances of various novel μVEDs designed for high power and broadband THz applications and achieved noticeable progresses on their microfabrication using advanced MEMS techniques. Although some technical challenges still remain, the accomplishments on this research will pave the way for achieving successful development of a Watt-level THz radiation source.

ACKNOWLEDGEMENT

This work is supported by Marine Corps Systems Command (MCSC), Grant No. M67854-06-1-5118.

References

[1] Young-Min Shin, Jin-Kyu So, Kyu-Ha Jang, Jong-Hyo Won, Anurag Srivastava, and Gun-Sik Park, Appl. Phys. Lett. 90, 031502 (2007)

[2] Young-Min Shin, Jin-Kyu So, Jong-Hyo Won, and Gun-Sik Park, Appl. Phys. Lett. 91, 031102 (2007)

[3] Young-Min Shin, Jin-Kyu So, Kyu-Ha Jang, Jong-Hyo Won, Anurag Srivastava, and Gun-Sik Park, Phys. Rev. Lett. 99, 147402 (2007)

[4] L. R. Barnett and Y. M. Shin, U.S. Patent Application No. 60/979,392 (12 October 2007)

[5] Young-Min Shin, and Larry R. Barnett, Appl. Phys. Lett. 92, 091501 (2008)

[6] Young-Min Shin, Larry R. Barnett, and Neville C. Luhmann Jr., IEEE Elec. Dev., submitted (2008)

[7] G. P. Scheitrum, G. Caryotakis, *et al.*, IEEE International Vacuum Electronics Conference Proceeding, 481, (2006)

[8] Young-Min Shin, Gun-Sik Park, Glenn P. Scheitrum, and Bernard Arfin, IEEE Trans. Plas. Sci. 31 (6), 1317 (2003)

[9] Young-Min Shin, Jin-Kyu So, Seong-Tae Han, Kyu-Ha Jang, Gun-Sik Park, Jong-Hyun Kim and Suk-Sang Chang, Appl. Phys. Lett. 88, 091916 (2006)